ISBN: 978-3-95450-227-1 ISSN: 2673-5490 doi:10.18429/JACoW-IPAC2022-MOPOTK045

GENERATION OF HIGH EMITTANCE RATIOS IN HIGH CHARGE ELECTRON BEAMS AT FACET-II*

O. Camacho†, UCLA Department of Physics and Astronomy, Los Angeles, CA, USA
A. Halavanau, R. Robles, Stanford University Department of Applied Physics
and SLAC National Accelerator Laboratory, Menlo Park, CA, USA

Abstract

Experiments foreseen at FACET-II, including dielectric plasma wakefield acceleration and linear collider tests, call for electron beams with highly asymmetric transverse emittances - so called "flat beams". A canonical recipe for the generation of such beams is injecting a magnetized beam at a waist into an appropriately tuned skewed quadrupole triplet channel. However, due to the intense non-linear space-charge forces that dominate nC bunches, this method presents difficulties in maintaining the flatness. We proceed with generalized round-to-flat-beam (RTFB) transformation, which takes into account the non-negligible divergence of the beam at the channel entrance, using a quartet of skewed quadrupoles. Our analytical results are further optimized in ELEGANT and GPT simulation programs and applied to the case of the FACET-II beamline. Non-ideal cathode spot distributions obtained from recent FACET-II experiments are used for accurate numerical modeling. Tolerances to quadrupole strengths and alignment errors are also considered, with an eye towards developing hardware specifications.

INTRODUCTION

Beam transport in PWA schemes is susceptible to transverse wakefields excited by particles far from the nominal axis. These wakefields have the potential to induce instabilities that spoil or even disintegrate the beam, and their presence therefore presents a strict limiting factor on the distances over which bunches can be immersed in intense accelerating gradients. It has been shown [1], [2] however, that such instabilities may be mitigated by employing a combination of a horizontal slab geometry in the accelerating structure and a matching transverse beam distribution. That is, an asymmetric flat beam. At a waist, $\sigma_i \sim \epsilon_i$, so that the product $\sigma_x \sigma_y \sim \epsilon_\perp$ is fixed, while the ratio $\frac{\sigma_x}{\sigma_y}$ ought to be maximized. Optimal stability requires that emittance from one transverse phase space plane be transferred into the other, thus achieving the desired asymmetry condition while respecting preservation of 4D emittance. This is achieved by exploiting conservation of canonical angular momentum $\mathbf{L_c} = \mathbf{r} \times (e\mathbf{A} + \mathbf{p})$. Imparting a beam with angular momentum, then removing, one can produce a beam which is much larger in one transverse dimension than the other, as desired. Real experimental conditions, of course, cause deviation from this ideal target. We therefore deem it worthwhile to benchmark error tolerance to ensure that the optimum found is a relatively stable one.

Modeling the FACET-II Injector

The highly nonlinear dynamics involved in modeling the emission and acceleration of a high-charge bunch necessitate a full 3-d treatment of space-charge and image-charge effects, for which the General Particle Tracer (GPT) code [3] is well suited. The bunch and low-energy beamline are therefore modeled in GPT; once the beam energy reaches 134 MeV, space-charge forces are sufficiently suppressed to permit the use of the ELEGANT [4] tracking code for further optimizations. The beam spot on the cathode is generated from experimentally measured images of the UV laser spot to be used at FACET-II to ensure fidelity between the dynamics in simulation and experiment.

In practice, the initial canonical angular momentum of the beam is supplied by immersing the cathode in an axial magnetic field $B_{z,M}$, provided by a solenoid around a 1.5 cell S-band photo-gun. Upon exiting the gun at an energy of 6 MeV, the beam is then focused by a second solenoid located in a drift space between the photo-gun exit and first travelling wave accelerating structure, the so-called L0AF, about 1.10 m from the cathode. The phase of the L0AF is optimized to simultaneously minimize the beam energy spread and normalized transverse emittance at its exit. The beam energy upon traversing this structure is brought up to 64 MeV.

Table 1: Injector Parameters

Symbol	Description	Value
$\epsilon_{\perp,0}$	Thermal emittance	3.3 mm-mrad
$B_{z,M}$	Magnetization solenoid	0.265 T
$B_{z,f}$	Focusing solenoid	0.189 T
$E_{z,g}$	Peak gun field	125 MV/m
ϕ_g	Gun launch phase	0 deg
$E_{z,L0AF}$	L0AF average accelerating gradient	20 MV/m
ϕ_{L0AF}	L0AF phase	0 deg
$E_{z,L0BF}$	L0BF average accelerating gradient	24 MV/m
ϕ_{L0BF}	L0BF phase	0 deg
E_f	Final bunch energy	134 MeV
$\epsilon_{n,\perp F}$	Final emittance	4.9 mm-mrad

The following accelerating structure (L0BF) is also phased to minimize emittance and energy spread, producing a 134 MeV beam with $\frac{\sigma_\gamma}{\bar{\gamma}} = 0.15$ % energy spread and 4.90 mm-mrad normalized emittance. This is the beam we match

* This work is supported by the U.S. Department of Energy Office of Science under Contract No. DE-AC02-76SF00515
† laotraemail14@gmail.com

ISBN: 978-3-95450-227-1 ISSN: 2673-5490 doi:10.18429/JACoW-IPAC2022-MOPOTK045

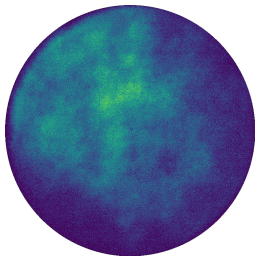

Figure 1: Typical intensity profile measured from FACET-II UV Laser.

into the skew-quadrupole channel that effects the RTFB transformation.

Analytical Estimates for RTFB Parameters

In the ideal case of a perfectly symmetric (round) beam injected into a skew quadrupole has been treated, for example, by Sun [5]. Given that the beam has initial covariance matrix Σ_0, the problem reduces to that of finding a sequence of magnetic elements and drifts with transfer matrix M_T such that $\Sigma_f = M_T \Sigma_0 M_T^T$ is block diagonalized. When this is done, the so-called "eigen-emittances" $\epsilon\pm$ of Σ_0 are projected onto the physical emittances ϵ_x, ϵ_y. $\epsilon_\pm = \epsilon_{n,0} \pm \mathcal{L}$, where $\mathcal{L}$ is the beam magnetization, proportional to the axial magnetic field on the cathode, and $\epsilon_{n,0}$ is the normalized rms emittance of the beam before the transformer. While this quantity is nominally preserved through transport, nonlinearities and small residual couplings may perturb $\epsilon_{n,0}$. Suns formulas for the requisite quadrupole strengths q_i in the thin-lens limit are quoted below. They are derived further assuming interquad drifts L_1, L_2 and a round beam with $\beta_x = \beta_y = \beta$ and $\alpha_x = \alpha_y = \alpha$.

$$
\begin{aligned}
q_1 &= \pm\sqrt{\frac{D(\alpha,\beta)}{\beta}} \\
q_2 &= -\frac{L_T\alpha - \beta}{L_1 L_2 (1 - \beta q_1)} \\
q_3 &= \frac{\beta(q_1 + q_2 - \alpha\beta L_1 q1 q2) + 1 + \alpha^2}{\beta(1 - \alpha(L_T q_1 + L_2 q_2)) + L_1 L_2 q2}
\end{aligned}
\tag{1}
$$

Where $D(\alpha,\beta) = 1 + \alpha^2 + \frac{\beta^2}{L_1 L_T} - \alpha\beta(\frac{L_1+L_T}{L_1 L_T})$, $L_T = L_1 + L_2$, and the sign ambiguity corresponds to the choice of whether the final beam is flattened horizontally or vertically.

The General Case of an Asymmetric Beam

In practice, perfect cylindrical symmetry of the incoming beam cannot be guaranteed, and imperfections in the photoemission profile (Fig. 1) and beamline element alignments will conspire to introduce deviations from it. Mathematically, this introduces an additional degree of freedom into the expressions for the off-diagonal elements of the post-lattice beam matrix Σ_f, corresponding to the need for an additional drift-quadrupole pair in the lattice to fully remove the remaining phase-space cross correlations. While it is in principle possible to derive a four quadrupole generalization of Eqs. (1), the resulting expressions are analytically unwieldy. In any case, deviations from symmetry are usually sufficiently small that we can consider them to be a perturbation to a nominally symmetric solution. In our case, for example, $\frac{\sigma_x}{\sigma_y} \approx 1.09$ at the transformer entrance. In light of this, the procedure we opt for is seeding numerical optimizations with the values of q_1, q_2, and q_3 derived under the symmetry assumption and an initial value of $q_4 = 0$. We content ourselves with this solution right now, as it proves adequate for our studies, and leave the full theoretical treatment of flattening asymmetric beams to future work.

SIMULATION RESULTS

Optimizations based on this scheme were performed using third order transfer matrices in ELEGANT, before being benchmarked in GPT with 3-d space-charge (Fig. 2). The quadrupole gradients were chosen by minimizing the cross-correlations of Σ_f via a Nelder-Mead procedure seeded with values from (1). The longer drift between the QF2 and QF3 elements is chosen to accommodate the insertion of a laser-heating element to suppress instabilities arising from energy self-modulation. Along with the other quadrupole spacings, it was held constant during optimization. The results are presented below; as expected, the fourth quadrupole is quite weak compared to the other three. The required gradients are quite modest and well within the operating range of existing hardware. In general, allowing the beam sufficient space to expand inside the transformer allows one to achieve good shaping with weaker magnets. This is because, in the absence of space-charge, $B_\perp \sim |\mathbf{r}|$, so that for a beam with very small radial extent, aggressive focusing is required to impart a significant angular kick.

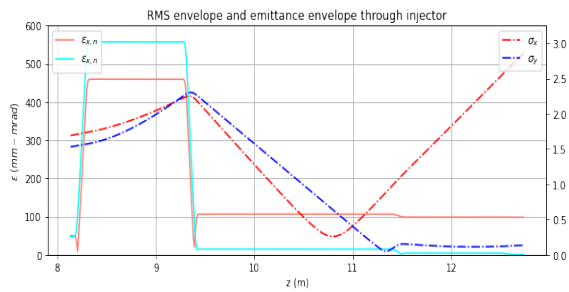

Figure 2: RMS width and emittance evolution for the two transverse planes of the beam during passage through the RTFB adapter.

The final ratio $\frac{\epsilon_x}{\epsilon_y}$ is an exceptional value of 290, with rms spot sizes satisfying $\frac{\sigma_x}{\sigma_y} \approx 20$ (Fig. 3). This level of asymmetry exceeds the criteria generally stipulated for flat beams in DWA, $\frac{\epsilon_x}{\epsilon_y} \approx 100$ and $\frac{\sigma_x}{\sigma_y} \approx 10$ [6].

ISBN: 978-3-95450-227-1 ISSN: 2673-5490 doi:10.18429/JACoW-IPAC2022-MOPOTK045

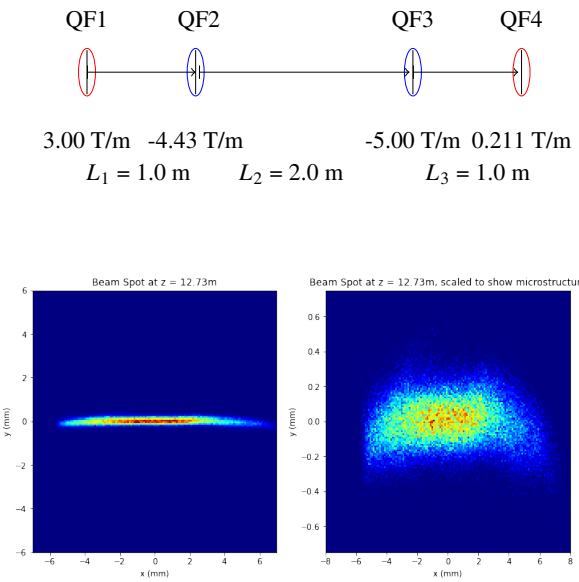

Figure 3: Schematic of transformer (top) and beam spot after quadrupole quartet (bottom).

EXPERIMENTAL FEASIBILITY

Beam Microstructure

Imperfections in the laser optics generating the UV spot on the cathode generate not an ideal flat-top, but a combination of high density"hot spots" and pockets of lower density, which are exaggerated by space-charge forces. The tight control on the transverse temperature of the beam achieved via emittance compensation and acceleration prevent this distribution from thermalizing, and these imperfections in the beam spot can be seen "frozen in" at the end of the transformer. The impact of such distribution imperfections upon acceleration and passage through a plasma channel have yet to be studied.

A closer look at the flattened beam profile in Fig. 3 confirms this, revealing low density flares along the spot and a notable rarefied tail for x > 3 mm. The beam also emerges with a slight nonlinear "C" shape. Further simulations will determine whether these effects have a notable impact on PWA performance.

Tolerance Studies

Experience has shown that the high emittance ratios achieved in numerical optimizations like our own are highly sensitive to perturbations of the parameters in experiment [7], especially at high charge. Results are likely to be impacted by small perturbations to the nominal quadrupole tilt angle and gradient. To estimate the performance of the system, we introduce 100 independent Gaussian distributed errors with mean zero and rms 0.2% to these parameters and report the resulting emittance ratio distribution.

One of the primary limiting factors observed in the study is the smaller of the two eigen-emittances, only 0.37 µm at

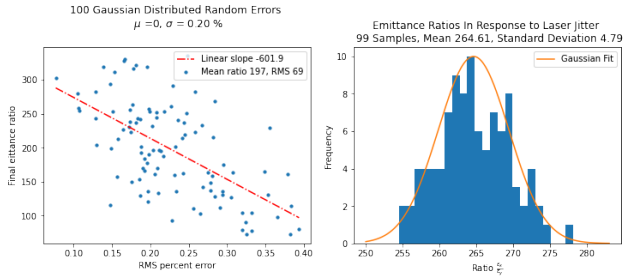

Figure 4: Final emittance ratios of beam in response to beamline (right) and laser errors(left).

the end of the transformer; even a sub-micron increase in this value can have a significant impact on the ratio $\frac{\epsilon_x}{\epsilon_y}$. However, the larger emittance $\epsilon_x \approx 100$ µm is quite stable, a fact which bodes well for the compression and acceleration of the beam in preparation for injection into plasma. The results suggest that, experimentally, we can expect to see not the extremely optimal value of $\frac{\epsilon_x}{\epsilon_y} = 290$, but the perturbation averaged value, closer to $\frac{\epsilon_x}{\epsilon_y} = 200$ (Fig. 4). This level of discrepancy between error-free and perturbation averaged results is consistent with experimental studies [8]

This naturally leads one to wonder whether a lattice optimized for a given cathode spot will be reliable shot to shot when variations in the laser distribution are taken into account. Fortunately, comparison of the evolution of cathode distributions obtained from multiple laser measurements shows small variation in the final beam matrix and corresponding emittance ratios. These data indicate that the primary source of error should be in beam transport rather than laser jitter at the cathode.

CONCLUSIONS

We have presented a preliminary study of high charge flat beam production at the FACET-II facility, seeding high accuracy simulations with experimental photo-gun laser data. Acceleration and emittance compensation of the space-charge dominated beam was modeled, optimizing the beamline 0.15% energy spread and 4.9 µm emittance. A four quadrupole scheme was employed to account for the deviations from ideal cylindrical symmetry, with beamline space for a laser-heating element allocated between quadrupoles. The transformed beam exhibits an emittance ratio more than adequate for applications. Tolerance studies on the optimal RTFB lattice are favorable, lending credence to the proposed production of high charge flat beams at FACET-II operating reliably within the performance range demanded by PWA experiments. Further studies on the impact of beam density fluctuations on transport through the FACET-II beamline and plasma injection will be necessary to further characterize the performance of this potentially fruitful line of research at FACET-II.

ISBN: 978-3-95450-227-1 ISSN: 2673-5490 doi:10.18429/JACoW-IPAC2022-MOPOTK045

REFERENCES

[1] A. Tremaine, J. Rosenzweig, and P. Schoessow, "Electromagnetic wake fields and beam stability in slab-symmetric dielectric structures ", *Phys. Rev. E*, vol. 56, p. 7204, Dec. 1997. doi:10.1103/PhysRevE.56.7204

[2] S.S. Baturin, G. Andonian, and J.B. Rosenzweig, "Analytical treatment of the wakefields driven by transversely shaped beams in a planar slow-wave structure", *Phys. Rev. Accel. Beams*, vol. 21, p. 121302, Dec. 2018. doi:10.1103/PhysRevAccelBeams.21.121302

[3] S. B. van der Geer and M. J. de Loos, "Applications of the General Particle Tracer Code", in *Proc. PAC'97*, Vancouver, Canada, May 1997, paper 8P090, pp. 2577–2579. doi:10.1109/PAC.1997.751279

[4] M. Borland, "Elegant: A Flexible SDDS-Compliant Code for Accelerator Simulation", Argonne National Lab., IL, USA, Rep. Photon Source LS-287, Aug. 2000. doi:10.2172/761286

[5] Y. Sun, "Angular-momentum dominated electron beams and flat-beam generation", Ph.D. thesis, University of Chicago, USA, Jun. 2005. doi:10.2172/15017103

[6] J. B. Rosenzweig *et al.*, "Physics Goals of DWA Experiments at FACET-II", in *Proc. IPAC'21*, Campinas, Brazil, May 2021, pp. 3922–3925. doi:10.18429/JACoW-IPAC2021-THPAB071

[7] A. Halavanau, S. J. Gessner, C. E. Mayes, and J. B. Rosenzweig, "Hollow and Flat Electron Beam Generation at FACET-II", in *Proc. IPAC'21*, Campinas, Brazil, May 2021, pp. 376–378. doi:10.18429/JACoW-IPAC2021-MOPAB101

[8] A. Halavanau, P. Piot, J. Hyun, D. Mihalcea, T. Sen, and J. C. T. Thangaraj, "Magnetized and Flat Beam Experiment at FAST", in *Proc. IPAC'17*, Copenhagen, Denmark, May 2017, pp. 3876–3879. doi:10.18429/JACoW-IPAC2017-THPAB073